

Melting of the critical behavior of a Tomonaga-Luttinger liquid under dephasing

Jean-Sébastien Bernier*,¹ Ryan Tan*,² Chu Guo,³ Corinna Kollath,¹ and Dario Poletti^{4,2,†}

¹*Physikalisches Institut, University of Bonn, Nussallee 12, 53115 Bonn, Germany*

²*Engineering Product Development Pillar, Singapore University of Technology and Design, 8 Somapah Road, 487372 Singapore*

³*Supremacy Future Technologies, Guangzhou 511340, China*

⁴*Science and Math Cluster, Singapore University of Technology and Design, 8 Somapah Road, 487372 Singapore*

Strongly correlated quantum systems often display universal behavior as, in certain regimes, their properties are found to be independent of the microscopic details of the underlying system. An example of such a situation is the Tomonaga-Luttinger liquid description of one-dimensional strongly correlated bosonic or fermionic systems. Here we investigate how such a quantum liquid responds under dissipative dephasing dynamics and, in particular, we identify how the universal Tomonaga-Luttinger liquid properties melt away. Our study, based on adiabatic elimination, shows that dephasing first translates into the damping of the oscillations present in the density-density correlations, a behavior accompanied by a change of the Tomonaga-Luttinger liquid exponent. This first regime is followed by a second one characterized by the diffusive propagation of featureless correlations as expected for an infinite temperature state. We support these analytical predictions by numerically exact simulations carried out using a number-conserving implementation of the matrix product states algorithm adapted to open systems.

I. INTRODUCTION

In equilibrium many-body systems, the insensitivity of large scale macroscopic observables to the microscopic details of the system is indicative of the emergence of universal behaviors [1]. For instance, such universal behavior is apparent in many one-dimensional systems where the low energy properties can be described by the Tomonaga-Luttinger liquid theory both for fermions and bosons [2]. Investigating the emergence of such behaviors is not restricted to equilibrium correlated systems. In fact, understanding how universality arises in out-of-equilibrium systems is both of fundamental and practical interest. For example, developing the next generation of quantum technologies will very likely require a thorough understanding of the response of large many-body quantum systems to both unitary and dissipative perturbations and drivings.

In this context, one important question relates to the robustness of the universal behavior of a Tomonaga-Luttinger liquid to environmental couplings. A direction pursued, for instance, in [3] where the evolution of a Tomonaga-Luttinger liquid in contact with a dephasing environment was considered using a Keldysh functional approach [4, 5], and in [6] where a Tomonaga-Luttinger liquid coupled quadratically to a finite temperature bath was studied. These works underline that it is now possible to consider the combined influence of universality and quantum dissipation on the non-equilibrium dynamics of strongly correlated systems. Theoretical predictions made from newly available numerical and analytical methods can even be tested in state-of-the-art ultracold atoms experiments. For example, ultracold atoms un-

der the effect of dephasing were studied in [7–9], and the dissipative dynamics of Rydberg atoms were investigated in [10–12].

On the theoretical side, one method has come to prominence to study many-body open quantum systems and relies on adiabatically eliminating fast decaying or decohering modes (see for instance [13–15]). This so-called adiabatic elimination technique was successfully applied to explain the nature of the dephasing dynamics of a bosonic gas, and led to the prediction of interaction-induced impeding. This phenomenon is characterized by the “slowing down” of a system relaxation dynamics due to the interplay of interaction, kinetic and dissipation effects [15]. This impeding can take various forms as it can give rise to emerging power-law [15, 16] and stretched exponential [17] relaxations, and can even lead to the occurrence of aging [18, 19]. In fact, the power-law relaxation dynamics predicted analytically by adiabatic elimination in [15, 17] has by now been observed experimentally in [9]. One should also note that impeded relaxation dynamics were also predicted to occur in the presence of disorder [20, 21] or kinetic constraints [22, 23].

In addition, important progress has recently been made to optimize the matrix product states (MPS) algorithm [24, 25] to study open quantum systems. While MPS has been used to investigate such dissipative systems for several years [25–28], a number-conserving algorithm for open quantum systems was only implemented recently (see e.g. [19, 29, 30]). For a certain class of systems, this approach was found to significantly reduce the size of the matrices that need to be manipulated, thus allowing one to consider larger systems.

Here we use both adiabatic elimination and a number-conserving MPS algorithm for open systems to study the relaxation dynamics of a Tomonaga-Luttinger liquid under the effect of dephasing. From adiabatic elimination, we predict that the spatial decay of the correlations is altered from its initial universal algebraic be-

*These authors contributed equally to the work.

†Electronic address: dario_poletti@sutd.edu.sg

havior and adopts the algebraic scaling expected for a non-interacting gas. At later times, a second regime diffusively takes over, and is characterized by featureless correlations corresponding to the infinite temperature state. We complement the adiabatic elimination study with quasi-exact numerical simulations based on a number-conserving MPS algorithm. Using this method, we study open quantum systems of up to 84 sites and 21 hard-core bosonic particles. Within the time interval numerically reachable, we find our simulations to be consistent with the predictions from adiabatic elimination. While the Tomonaga-Luttinger liquid long-range correlations appear to be maintained over short times, the propagation of a dissipation-induced perturbation can be clearly seen. We also detect a likely change of the algebraic exponent characterizing the spatial decay of the Tomonaga-Luttinger correlations.

The manuscript is structured in the following manner: In Sec. II, we introduce the model and describe the properties of the ground state of a system of hard-core bosons which we use as the initial condition for our study. In Sec. III, we provide an overview of the methods used: the adiabatic elimination technique and the matrix product states algorithm with number conservation applied to the study of open systems. In Sec. IV, we present how the Tomonaga-Luttinger-like properties are affected by the dephasing dynamics first using adiabatic elimination IV A, and then, in Sec. IV B, we show how these results are supported by numerically exact MPS simulations. We conclude in Sec. V.

II. MODEL

We study the effects of dephasing on the short time dynamics of hard-core bosons in an optical lattice. The Hamiltonian of the system is given by

$$\hat{H} = -J \sum_{l=1}^{L-1} (\hat{b}_l \hat{b}_{l+1}^\dagger + \hat{b}_l^\dagger \hat{b}_{l+1}) + V \sum_{l=1}^{L-1} \hat{n}_l \hat{n}_{l+1}, \quad (1)$$

where J is the hopping magnitude, V is the strength of the nearest-neighbour repulsion, L is the number of sites. Here we wrote down the Hamiltonian for open boundary conditions as will be considered in our numerical treatment using MPS methods. \hat{b}_l and \hat{b}_l^\dagger respectively annihilate and create a hard-core boson at site l . The operator $\hat{n}_l = \hat{b}_l^\dagger \hat{b}_l$ counts the number of hard-core bosons at site l , and due to the hard-core bosons conditions $\hat{b}_l^\dagger \hat{b}_l^\dagger = 0$, $\hat{n}_l = 0, 1$. We consider the evolution of the density operator $\hat{\rho}$ to be described by a Lindblad master equation [31–33] with local dephasing on all sites of the system,

$$\frac{d\hat{\rho}}{dt} = -\frac{i}{\hbar} [\hat{H}, \hat{\rho}] + \mathcal{D}(\hat{\rho}), \quad (2)$$

where the dissipator $\mathcal{D}(\hat{\rho})$ takes the form

$$\mathcal{D}(\hat{\rho}) = \gamma \sum_{l=1}^L 2\hat{n}_l \hat{\rho} \hat{n}_l - \hat{n}_l^2 \hat{\rho} - \hat{\rho} \hat{n}_l^2. \quad (3)$$

The jump operators \hat{n}_l , being Hermitian, drive the system towards the infinite temperature state which, given the interplay between the Hamiltonian and the dissipator, is the only steady state of the system. In fact, this dissipator is relevant to the study of ultracold atoms under the effect of fluorescent scattering [34, 35], and was also realized experimentally [7–9].

We prepare initially the system in the ground state of the Hamiltonian, Eq. (1), and then switch on the dissipation at $t > 0$. For the chosen fillings, $\bar{n} = \sum_l \langle \hat{n}_l \rangle / L$, and interaction strength, $0 \leq V \leq J$, the initial state is typically well described as a Tomonaga-Luttinger liquid [2, 36].

In order to facilitate the use of the many-body adiabatic elimination method, we rewrite the lattice system of hard-core bosons confined to an optical lattice and subjected to local dephasing noise to the spin-1/2 XXZ chain coupled to dephasing. Using the mapping,

$$\begin{aligned} \hat{b}_l^\dagger &\rightarrow \hat{S}_l^+, \\ \hat{b}_l &\rightarrow \hat{S}_l^-, \\ \hat{n}_l - \frac{1}{2} &\rightarrow \hat{S}_l^z, \end{aligned}$$

where \hat{S}_l^α is the α -direction spin operator at site l , together with the transformation

$$\begin{aligned} \hat{S}_l^+ &\rightarrow (-1)^l \hat{S}_l^+, \\ \hat{S}_l^- &\rightarrow (-1)^l \hat{S}_l^-, \\ \hat{S}_l^z &\rightarrow \hat{S}_l^z, \end{aligned}$$

the evolution of the density operator $\hat{\rho}$ can now be described by the Lindblad master equation

$$\frac{d\hat{\rho}}{dt} = -\frac{i}{\hbar} [\hat{H}_{\text{XXZ}}, \hat{\rho}] + \mathcal{D}_Z(\hat{\rho}).$$

Here, the XXZ Hamiltonian with periodic boundary conditions is

$$\hat{H}_{\text{XXZ}} = \sum_{l=1}^L \left[J \left(\hat{S}_l^+ \hat{S}_{l+1}^- + \hat{S}_{l+1}^+ \hat{S}_l^- \right) + V \hat{S}_l^z \hat{S}_{l+1}^z \right],$$

where J and V are the exchange couplings along the different spin directions, L is the length of the chain, and $\hat{S}_{L+1}^\alpha = \hat{S}_1^\alpha$. The dissipator takes the form

$$\mathcal{D}_Z(\hat{\rho}) = 2\gamma \sum_{l=1}^L \left(\hat{S}_l^z \hat{\rho} \hat{S}_l^z - \frac{1}{4} \hat{\rho} \right),$$

where γ is the dissipation strength. In this notation the dissipation induces spin fluctuations.

As we consider a situation where the system is initially prepared as a Tomonaga-Luttinger liquid, we briefly discuss the structure of the correlations associated with this state as they are used as inputs within adiabatic elimination. In this liquid, for $L \rightarrow \infty$, the spin correlations along the z -direction decay algebraically as

$$\langle \hat{S}_l^z(0) \hat{S}_{l+d}^z(0) \rangle = \left(\bar{n} - \frac{1}{2} \right)^2 + A_z (-1)^d \frac{\cos(qd)}{|d|^{1/\eta}} - \frac{1}{4\pi^2 \eta |d|^2} \quad (4)$$

where $q = 2\pi(\bar{n} - \frac{1}{2})$, $\eta = 1/(2K)$, with K the Tomonaga-Luttinger parameter, and A_z is a function of the interaction strength V [36]. As for finite interaction strengths, $V > 0$, the Tomonaga-Luttinger parameter $K < 1$, the term in $d^{-1/\eta} = d^{-2K}$ dominates. The correlations present oscillations whose period depends on the filling, and the leading corrections go as d^{-2} . These spin correlations can be mapped back to the density-density correlations as

$$\langle \hat{S}_l^z \hat{S}_{l+d}^z \rangle \rightarrow \langle \hat{n}_l \hat{n}_{l+d} \rangle - \bar{n} + \frac{1}{4}.$$

Theoretically, this dissipative system has been the subject of a number of studies. The evolution of various equal-time correlations were investigated in [16] whereas two-time density-density correlations, or equivalently spin-spin correlations, were considered in [19].

III. METHODS

In this work we employ two complementary approaches. First, we use an approximate approach based on many-body adiabatic elimination [13–15] to build up an analytical understanding of the correlation propagation regimes encountered at intermediate to long times. This method is described in Sec.III A. While adiabatic elimination provides deep insights into the evolution of this correlated system under the effect of dephasing, it does not correctly capture the initial propagation dynamics and does not assign the appropriate timescales to the different regimes. To fill some of these gaps, we compute the short to intermediate time evolution of our system using a matrix product state (MPS) algorithm [25] for open systems. This quasi-exact numerical method allows for accurate estimations of the computational error which, in principle, can be made arbitrarily small. We describe this approach in Sec.III B.

A. Adiabatic Elimination

To gain analytical insights into the evolution of the system, we employ many-body adiabatic elimination. This method relies on the observation that, for sufficiently large times and irrespective of the system parameters,

the dissipation-free subspace will be reached. While this subspace is highly degenerate with respect to the dissipator, the Hamiltonian lifts this degeneracy. Performing adiabatic elimination helps identifying how virtual excitations around the dissipation-free subspace affect the system dynamics.

For the system considered here, the dissipation-free subspace formed by all $\hat{\rho}_0$ for which $\mathcal{D}_Z(\hat{\rho}_0) = 0$, takes the form $\hat{\rho}_0 = \sum_{\vec{\sigma}} \rho_{0,\vec{\sigma}} |\vec{\sigma}\rangle \langle \vec{\sigma}|$ where the different spin configurations are labeled within the z -component basis such that $\vec{\sigma} = (\sigma_1, \sigma_2, \dots, \sigma_L)$ with $\sigma_l = \pm 1/2$. Adiabatic elimination allows one to describe the effective dynamics within this subspace by considering the effect induced by virtual excitations. As described in [19], for times larger than $1/\gamma$, the evolution of the different elements of the density matrix is effectively described by the set of differential equations

$$\frac{\partial \rho_{0,\vec{\sigma}}}{\partial t} = \sum_{l=1}^L \frac{J^2 \gamma}{[(V \alpha_{\vec{\sigma},l})^2 + (\hbar \gamma)^2]} \delta_{\sigma_l, \bar{\sigma}_{l+1}} (\rho_{0,\vec{\sigma}_l} - \rho_{0,\vec{\sigma}}),$$

where $\alpha_{\vec{\sigma},l} = (\sigma_{l-1} \sigma_l + \sigma_{l+1} \sigma_{l+2})$, $\bar{\sigma}_l$ is the spin configuration $\vec{\sigma}$ with swapped spins at site l and $l+1$.

We then use this set of differential equations for ρ_0 to write down a set of coupled differential equations for the spin correlations $\mathcal{C}_{l,l+d}(t) = \langle \hat{S}_l^z(t) \hat{S}_{l+d}^z(t) \rangle$. Together with periodic boundary conditions, these equations, valid for $\hbar \gamma \gg V$ (as these expressions were obtained by formally taking the limit $V \rightarrow 0$), take the form

$$\begin{aligned} \frac{\partial}{\partial t} \mathcal{C}_{j,j\pm 1} &= D (\mathcal{C}_{j\mp 1,j\pm 1} + \mathcal{C}_{j,j\pm 2} - 2 \mathcal{C}_{j,j\pm 1}), \\ \frac{\partial}{\partial t} \mathcal{C}_{j,j+d} &= D (\mathcal{C}_{j+1,j+d} + \mathcal{C}_{j-1,j+d} + \mathcal{C}_{j,j+d+1} \\ &\quad + \mathcal{C}_{j,j+d-1} - 4 \mathcal{C}_{j,j+d}), \quad \text{for } |d| > 1, \end{aligned}$$

where $D = J^2/(\hbar^2 \gamma)$ and we dropped here the time from $\mathcal{C}_{l,l+d}(t)$ to simplify the notation. As the system is initially prepared as a Tomonaga-Luttinger liquid, the correlations are translationally invariant, $\mathcal{C}_d(t) = \mathcal{C}_{j,j+d}(t)$, such that the system of equations can be simplified to

$$\begin{aligned} \frac{\partial}{\partial t} \mathcal{C}_{\pm 1} &= 2D (\mathcal{C}_{\pm 2} - \mathcal{C}_{\pm 1}), \\ \frac{\partial}{\partial t} \mathcal{C}_d &= 2D (\mathcal{C}_{d+1} + \mathcal{C}_{d-1} - 2 \mathcal{C}_d), \end{aligned} \quad (5)$$

where, for the second equation, $-L/2 + 1 \leq d < -1$ or $1 < d \leq L/2$.

To solve this system of differential equations for which $\mathcal{C}_d(t) = \mathcal{C}_{-d}(t)$, it is convenient to redefine the correlations such that the evolution for all distances is described by differential equations of the same form. To do so, we redefine the correlations as $\tilde{\mathcal{C}}_d(t) = \mathcal{C}_d(t)$ for $1 \leq d \leq L/2$ and $\tilde{\mathcal{C}}_{d+1}(t) = \mathcal{C}_d(t)$ for $-L/2 + 1 \leq d \leq -1$ implying that $\tilde{\mathcal{C}}_d(t) = \tilde{\mathcal{C}}_{-d+1}(t)$ for $1 \leq d \leq \frac{L}{2}$. One can then write down a diffusion equation for $\tilde{\mathcal{C}}_d$ with diffusion constant

D

$$\frac{\partial}{\partial t} \tilde{C}_d = 2D \left(\tilde{C}_{d+1} + \tilde{C}_{d-1} - 2 \tilde{C}_d \right)$$

valid for $-L/2 + 2 \leq d \leq L/2$.

This differential equation can be solved analytically in terms of the modified Bessel functions $I_n(x)$, and has for solution

$$\tilde{C}_d(t) = \left(\bar{n} - \frac{1}{2} \right)^2 + e^{-4Dt} \left(\sum_{d'=1}^{L/2} C_{d'}(0) I_{d'-d}(4Dt) + \sum_{d'=1}^{L/2-1} C_{d'}(0) I_{d'+d-1}(4Dt) \right), \quad (6)$$

where $C_d(0) = \langle S_l^z(0) S_{l+d}^z(0) \rangle$ are the spin correlations in the z -direction. For $d \geq 1$, in the limit where $L \gg 1$, the correlations can be written as

$$C_d(t) = \left(\bar{n} - \frac{1}{2} \right)^2 + e^{-4Dt} \left(\sum_{d'=1}^{\infty} C_{d'}(0) [I_{d'-d}(4Dt) + I_{d'+d-1}(4Dt)] \right). \quad (7)$$

Using the initial conditions given by Eq. (4), it is instructive to consider two limits. For $d > \sqrt{4Dt}$, we find that these correlations are well approximated by the expression

$$C_d(t) = \left(\bar{n} - \frac{1}{2} \right)^2 + A_z \frac{(-1)^d}{d^{1/\eta}} e^{-4Dt(1+\cos q)} \cos(qd) - \frac{1}{4\pi^2\eta} \frac{1}{d^2}, \quad (8)$$

where A_z is a constant. This result suggests that the algebraic decay characterized by the Tomonaga-Luttinger liquid exponent and the associated oscillations are damped out on a timescale set by $4D(1+\cos q)$. However, one should note that the validity of these results at short times need to be confirmed using more robust methods as, initially, the system might not be close enough to the dissipation-free subspace. For longer times, as only the term in $d^{-1/\eta}$ is damped, the correlations will remain algebraic for distances larger than $\sqrt{4Dt}$, but their scaling exponent will change. In fact, irrespective of the initial interaction strength V , there exists a certain intermediate regime, in distance and time, where the correlations will scale as d^{-2} .

At very long times, the correlations become uniform over all distances and their value varies as

$$C_d(t) = \left(\bar{n} - \frac{1}{2} \right)^2 + \frac{1}{\sqrt{2\pi Dt}} S_0, \quad (9)$$

where

$$S_0 = \frac{A_z}{2} \left(\text{Li}_{\frac{1}{\eta}}(-e^{-iq}) + \text{Li}_{\frac{1}{\eta}}(-e^{iq}) \right) - \frac{1}{24\eta},$$

with $\text{Li}_n(x)$, the polylogarithm function. One sees here that the correlations along the z -direction approach their final value $(\bar{n} - 1/2)^2$ following a scaling $t^{-1/2}$. We detail further the evolution of these correlations in Sec. IV A where we discuss the results obtained within the adiabatic elimination formalism.

B. Matrix Product States

Simulating exactly the time evolution of interacting lattice bosons under the effects of dephasing would require a very large amount of memory since we are dealing with density matrices which require the square of the elements needed when considering wavefunctions. In order to circumvent this problem, we use a number-conserving MPS algorithm adapted to dissipative systems. We reshape the density matrix to a vector which we then represent within the MPS formalism (for the first works in this direction, although without number conservation, see [26, 27]). Methods based on matrix product states rely on rewriting a quantum states as [25]

$$|\psi\rangle = \sum_{\sigma_1 \dots \sigma_L} F^{\sigma_1} \dots F^{\sigma_L} |\sigma_1 \dots \sigma_L\rangle, \quad (10)$$

where σ_l represents the physical degree of freedom on the l -th site. For a system with a $U(1)$ symmetry, e.g. particle number conservation, each F^{σ_l} can be taken as a matrix $F_{(a_l, \alpha_l), (a_{l+1}, \alpha_{l+1})}^{\sigma_l}$, with auxiliary indices a_l and a_{l+1} , and labelled by quantum numbers α_l and α_{l+1} . In the case of a sufficiently large matrix dimension, the representation of the state is exact. The idea which makes the MPS methods feasible is the truncation of the maximum sizes of the auxiliary dimensions using singular value decompositions, while the quantum numbers are constrained by $\alpha_l + \sigma_l = \alpha_{l+1}$, with $\alpha_L = N$, where N is the total number of atoms.

In order to deal with density matrices, we rewrite $\hat{\rho} = |\psi\rangle\langle\psi|$ as a vector $|\rho\rangle\rangle$, and then in close analogy as for the vector that describes a quantum state, we can write

$$|\rho\rangle\rangle = \sum_{\substack{\sigma'_1 \dots \sigma'_L \\ \sigma'_1 \dots \sigma'_L}} M^{\sigma_1 \sigma'_1} \dots M^{\sigma_L \sigma'_L} |\sigma_1 \sigma'_1 \dots \sigma_L \sigma'_L\rangle\rangle, \quad (11)$$

where now the system has a $U(1) \otimes U(1)$ symmetry. The l -th site is, more precisely, represented by the tensor $M_{(b_l, \alpha_l, \alpha'_l), (b_{l+1}, \alpha_{l+1}, \alpha'_{l+1})}^{\sigma_l \sigma'_l}$ where $\alpha_l + \sigma_l = \alpha_{l+1}$ and $\alpha'_l + \sigma'_l = \alpha'_{l+1}$ to ensure number conservation, while b_l and b_{l+1} are auxiliary indices. Here σ'_l indicates the physical degree of freedom on the l -th site of the bra of the density operator. The average value of a generic observable \hat{O} is computed as $\langle \hat{O} \rangle = \text{tr}(\hat{O} \hat{\rho})$, which can be rewritten for the vectorized $|\rho\rangle\rangle$ as $\langle \hat{O} \rangle = \langle \langle \mathbb{1} | \hat{O} | \rho \rangle \rangle$, where $|\mathbb{1}\rangle\rangle$ is the vectorized identity operator labelled with the same symmetries as $|\rho\rangle\rangle$.

At the initial time, the MPS $M^{\sigma_l \sigma'_l}$ for the density matrix are converted from the MPS in Eq.(10) which

represent the ground state by the following relation

$$M_{(b_l, \alpha_l, \alpha'_l), (b_{l+1}, \alpha_{l+1}, \alpha'_{l+1})} = F_{(a_l, \alpha_l), (a_{l+1}, \alpha_{l+1})}^{\sigma_l} \otimes F_{(a'_l, \alpha'_l), (a'_{l+1}, \alpha'_{l+1})}^{\sigma'_l}.$$

In our calculation we consider a bond dimension χ , given by the sum of all the local auxiliary indices b_l , of up to 8000 levels, and we remove singular values smaller than $\varepsilon = 10^{-7}$. In order to ensure that the ground state is well represented after conversion to the density operator $\hat{\rho}$, we have evolved $\hat{\rho}$ in absence of dephasing, i.e. $\gamma = 0$, to a time $Jt/\hbar = 1$ and verified that observables such as local density and local fluctuations remain constant up to an absolute accuracy of 10^{-9} .

This way of setting up the MPS representation of $|\rho\rangle\rangle$ allows one to write Eqs.(2) and (3) in order to calculate the time-evolution using

$$\frac{d|\rho\rangle\rangle}{dt} = \mathcal{L}|\rho\rangle\rangle \quad (12)$$

with the superoperator \mathcal{L} given by

$$\mathcal{L} = -\frac{i}{\hbar} \left(\hat{H} \otimes \hat{\mathbf{1}} - \hat{\mathbf{1}} \otimes \hat{H} \right) + \gamma \sum_l \left(2\hat{n}_l \otimes \hat{n}_l - \hat{n}_l^2 \otimes \hat{\mathbf{1}} - \hat{\mathbf{1}} \otimes \hat{n}_l^2 \right). \quad (13)$$

Note that the operators \hat{H} and \hat{n}_l are symmetric, and hence we do not need to take the transpose of the operators which would be acting on the bra.

Given the representation chosen for $|\rho\rangle\rangle$ in Eq.(11), with MPS taking into account the local indices of the ket and bra, respectively σ_l and σ'_l , Eqs.(12) and (13) result in operators acting only locally, or only coupling two nearest neighboring sites. We can thus decompose $\mathcal{L} = \mathcal{L}_E + \mathcal{L}_O$ where \mathcal{L}_E and \mathcal{L}_O act, respectively, only on the even or the odd bonds. We can then approximate the evolution of the density matrix over a small time interval dt using a fourth-order Trotter decomposition [37], which can be implemented using standard time-evolution MPS techniques, see for instance [25].

IV. RESULTS

A. Dephasing dynamics within adiabatic elimination

Investigating within adiabatic elimination the dissipative evolution of the density-density correlations, or correspondingly, for the XXZ Hamiltonian, the spin correlations along the z -direction, we identify two distinct regimes. Considering Eq. (7), one sees that these correlations are functions of the dimensionless time Dt where D is the diffusion constant defined earlier as $D = J^2/(\hbar^2\gamma)$. We therefore use this quantity to delineate the different regimes. While adiabatic elimination is unlikely to

capture the exact timescales as it notoriously underestimates the coherence initially present in the system, we can be fairly confident that for $t \gg 1/\gamma$, or in other words $Dt \gg [J/(\hbar\gamma)]^2$, this approach provides a faithful description of the dynamical regimes occurring under the effect of dephasing.

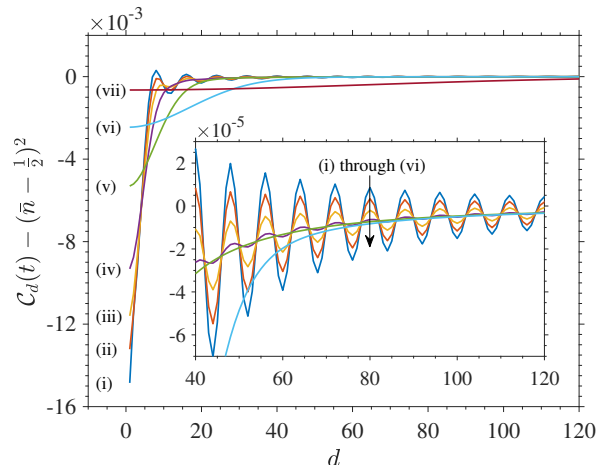


FIG. 1: Spin correlations along the z -direction, $C_d(t)$, for a system of length $L = 2000$, filling $\bar{n} = 1/8$, initial interaction strength $V = J$, and dissipative strength $\hbar\gamma = 5J$ corresponding to $\hbar^2 D = 0.2J^2$. The curves represent (i) $Dt = 0$, (ii) $Dt = 0.34$, (iii) $Dt = 0.95$, (iv) $Dt = 2.44$, (v) $Dt = 11.24$, (vi) $Dt = 62.98$, (vii) $Dt = 995.54$. Inset: same labelling as in the main figure, curves (i) to (vi) are ordered from top to bottom, curve (vii) is not shown. The spatial oscillations of the Tomonaga-Luttinger correlations are damped under the effect of dephasing. The correlations are obtained by numerically solving the set of differential equations, Eqs. (5).

For short to intermediate dimensionless times, we find that the algebraic decay of the correlations is maintained for all distances, albeit with decreased amplitude and changing exponent. Considering Eq. (8), valid for $d > \sqrt{4\pi Dt}$, one can see that for small Dt the term in $d^{-1/\eta}$ is only weakly damped such that the correlations are still dominated by the same algebraic term, and continue to present oscillations albeit with reduced amplitude. As time progresses, the window over which Eq. (8) does not apply widens and, in fact, the initial correlation structure completely melts away in this region. For $d \leq \sqrt{4\pi Dt}$, the correlations adopt a flat plateau-like structure described by Eq. (9) and the plateau height decreases in time as $t^{-1/2}$. In contrast, for $d > \sqrt{4\pi Dt}$, the correlations still decay algebraically but with a different exponent: the first term is completely damped out due to dephasing while the second term, in d^{-2} , remains unaffected. We present in more details these two regimes below using different graphical representations.

Focusing first on the short to intermediate distance behavior, one sees from Fig. 1 that the spatial oscillations present in the initial Tomonaga-Luttinger liquid correlations are damped under the effect of dephasing.

For larger Dt , at small distances one can notice a slow build-up as the correlations approach their final value $(\bar{n} - 1/2)^2$. In Fig. 1, this build-up and the melting of the algebraically decaying character is seen to propagate to larger correlation distances with increasing time.

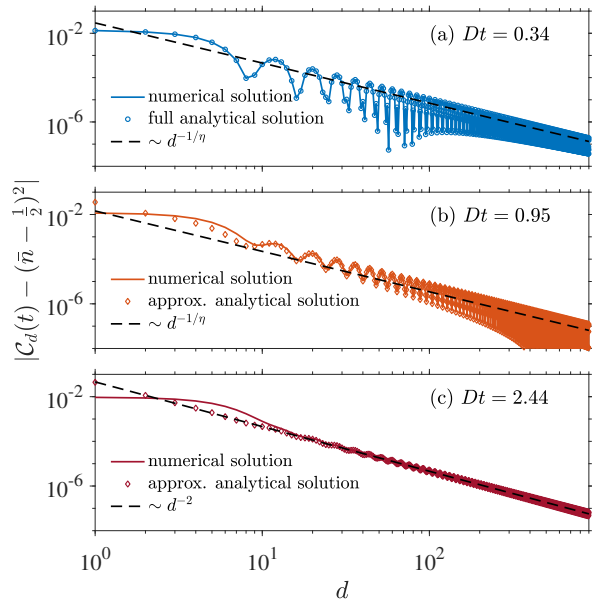


FIG. 2: Spatial scaling of the spin correlations along the z -direction, $C_d(t)$, for short to intermediate times. The same system parameters as in Fig. 1 are used. In (a), the numerical solution (solid line) is compared to the analytical solution (circle markers), Eq. (6). In (b) and (c), the numerical solution (solid line) is compared to the simplified expression, Eq. (8) (diamond markers).

Useful information about the evolution of the system can be extracted by considering the correlations over longer distances. At early times, as shown in Fig. 2 (a) and (b), the correlations in the tail scale as $d^{-1/\eta}$ as expected from Tomonaga-Luttinger theory. However, for increasing times, as seen in (c), the scaling changes to d^{-2} . This behavior is in agreement with Eq. (8), an approximated expression for $C_d(t)$, valid for $d > \sqrt{4\pi Dt}$ which, as explained earlier, highlights that only the $d^{-1/\eta}$ term is exponentially damped while the d^{-2} is unaffected. In Fig. 2, we further compare the correlations obtained from numerically solving the set of differential equations, Eqs. (5), to two analytical solutions Eqs. (6) and (8). In panel (a), one sees that the correlations obtained from the full analytical solution, Eq. (6), (circle markers) agree perfectly with the numerical solution (solid line). Whereas, in panels (b) and (c), one can see that the simplified analytical expression, Eq. (8), (diamond markers) captures very well the correlations for $d > \sqrt{4\pi Dt}$.

For larger Dt , a second regime sets in. In this regime, the correlations initial algebraic decay is completely obliterated for $d \leq \sqrt{4\pi Dt}$. For these distances, the amplitude of the correlations becomes spatially uniform and is only a function of time. As shown in Fig. 3,

the range of distances over which the correlations are featureless increases as a function of time, and their amplitude decreases as $t^{-1/2}$ towards their steady-state value of $(\bar{n} - 1/2)^2$ as described by Eq. (9). Beyond this propagation front, the spin correlations along the z -direction still scale as d^{-2} as found in the previous regime.

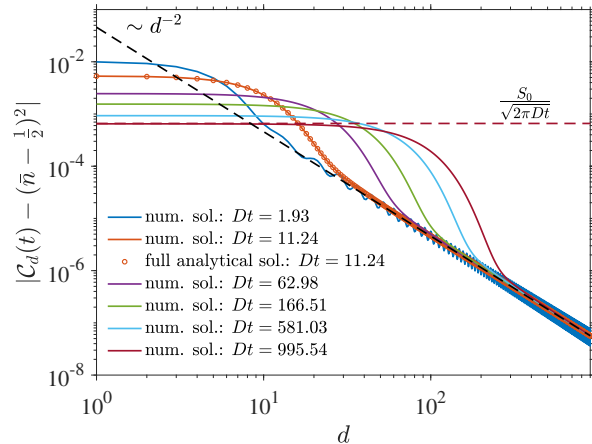


FIG. 3: Appearance, at longer times, of a second regime characterized by spatially uniform correlations. The same system parameters as in Fig. 1 are used. The curves are labelled in order of appearance at $d = 1$ from top to bottom. The value of the correlation plateau scales as $t^{-1/2}$, and beyond the propagation front the correlations scale as d^{-2} . For $Dt = 11.24$, one sees that, in this second regime, the correlations obtained from Eq. (6) (circle markers) also agree perfectly with the numerical solution (solid line).

As alluded to earlier, when considering Fig. 1, the algebraically decaying character of the correlations melts away over larger distances as time progresses. We want to understand here the mechanism by which the initial algebraically decaying correlation structure is being replaced by spatially uniform correlations under the effect of dissipation. To do so, one can notice from Fig. 3 that, for a given distance, $|C_d(t) - (\bar{n} - 1/2)^2|$ is maximal around the time when the propagation front, the flat region boundary, reaches this distance. The time-dependence of the spin correlations along the z -direction for $3 \leq d \leq 50$ is shown in Fig. 4. The correlations peak at the passage of the front, at a value we denote as t_{\max} , and then decay algebraically, as $t^{-1/2}$, towards their steady-state value, $(\bar{n} - 1/2)^2$. Plotting d as a function of Dt_{\max} , as presented in the inset of Fig. 4, one sees that the front propagates as $d \sim \sqrt{Dt_{\max}}$. This result indicates that the second regime, characterized by featureless correlations, propagates diffusively through the system. In other words, the regime characterized by algebraically decaying correlations disappears through the action of a diffusive process.

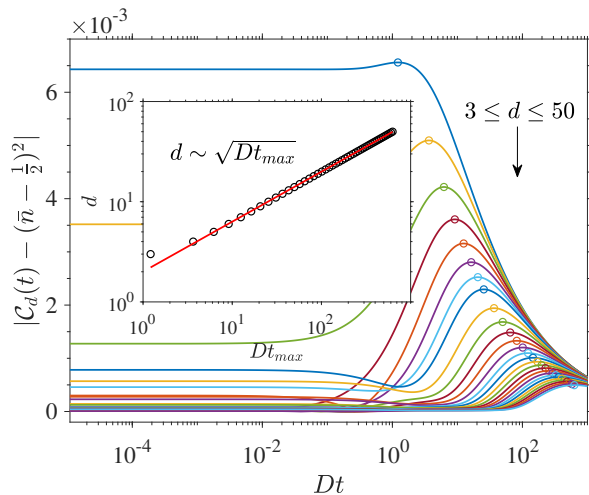


FIG. 4: Evolution of the spin correlations along the z -direction, $C_d(t)$, as a function of time for $3 \leq d \leq 50$ (from the right, top to bottom). The same system parameters as in Fig. 1 are used. For each distance, a circle marks the time, t_{\max} , at which the correlations are maximum. This maximum corresponds to the passage of the propagation front separating the regions displaying uniform and algebraically decaying correlations. Inset: the front propagates diffusively as $d \sim \sqrt{Dt_{\max}}$.

B. Dephasing dynamics within matrix product states

As explained in the previous section, adiabatic elimination underestimates the coherence initially present in the correlated system. Consequently, in order to put our previous results on a more solid ground, particularly the regime identified at short times, we conduct full-fledged MPS simulations on systems with fillings $\bar{n} = 1/8$, 11 bosons on 88 sites, and $\bar{n} = 1/4$, 21 bosons on 84 sites, and focus on the evolution of the density profile and density-density correlations.

Using this approach, we investigate the fate of the Tomonaga-Luttinger liquid as the system is subjected to dephasing, and consider times up to $tJ = 5\hbar$. We first consider the evolution of the density profiles. In Fig. 5 we present the density of the atoms $\langle \hat{n}_l \rangle$ as a function of the site l both for $1/4$ filling, panels (a) and (b), and filling $1/8$, panels (c) and (d). We consider both hard-core bosons without nearest-neighbor interaction, $V = 0$ in panels (a) and (c), and with interaction strength $V = J$ in panels (b) and (d). Each line corresponds to a different time, namely $tJ = 0$ for the blue dashed line, $tJ = 3\hbar$ for the orange dash-dotted line and $tJ = 5\hbar$ for the violet solid line. Note that we only show half the system, as the other half is mirror-symmetric. In Fig. 5, we observe that the initial density profile has a strong oscillatory behavior. One can notice that their amplitude is larger when the nearest-neighbor interaction is finite, and that their period is shorter for larger fillings. The presence of these Friedel oscillations is due to the use of open-

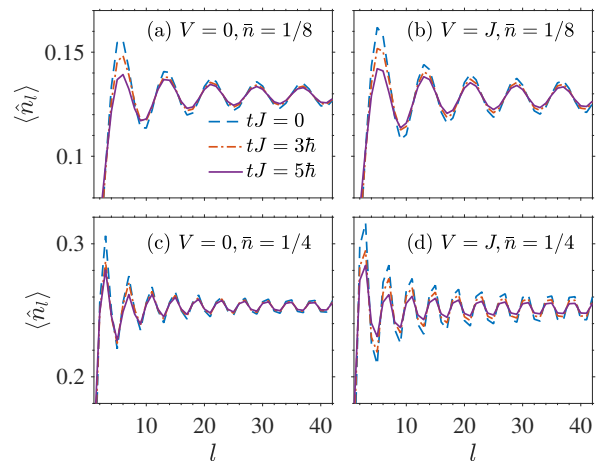


FIG. 5: Local density $\langle \hat{n}_l \rangle$ versus site number l , for different times: $tJ = 0$ (blue dashed line), $tJ = 3\hbar$ (orange dash-dotted line) and $tJ = 5\hbar$ (violet solid line). Panels (a) and (b) are for filling $\bar{n} = 1/8$ ($L = 88$, $N = 11$), $V = 0$ and $V = J$; (c) and (d) are for filling $\bar{n} = 1/4$ ($L = 84$, $N = 21$), $V = 0$ and $V = J$. For all panels $\hbar\gamma = 0.05J$ corresponding to $\hbar^2 D = 20J^2$. The amplitude of the density oscillations are damped due to dephasing. Results obtained via MPS simulations with $\chi = 8000$, $dtJ = 0.01\hbar$ and cut-off $\varepsilon = 10^{-7}$.

boundary conditions, and their structure at $t = 0$ is in excellent agreement with the density profile expected for a finite-size Tomonaga-Luttinger liquid. In an intermediate region slightly away from the system edge the initial density profile follows the expected expression

$$\langle \hat{n}_l \rangle = \frac{1}{2} + \frac{q}{2\pi} + \sqrt{2A_z} (-1)^l \frac{\sin(ql)}{(2l)^{1/(2\eta)}}$$

where, for a finite size system, $q = 2\pi \frac{L}{L+1} (\bar{n} - \frac{1}{2})$ [36], implying that the decay of the Friedel oscillations is dominated by the Tomonaga-Luttinger exponent.

As the dephasing dynamics sets in, the oscillations start to damp out, but the time-evolved density profiles appear to overall retain their initial shape. Motivated by this observation, we analyze further whether the evolution of the density profile keeps indeed a self-similar dependence on position. To check if this is the case, we rescale each profile within a given parameter set using the following procedure: we subtract from each profile the density at which all three profiles of the set intersect, we then divide each newly obtained profile by a single density, chosen from a site in the bulk of the system, for its maximal value. The result of this simple shift and rescaling is presented in Fig. 6. One can see that the profiles at different times collapse onto a single curve for sites slightly away from the edges. As the initial profile is the ground state density configuration for a Tomonaga-Luttinger liquid, our results support that the functional form predicted by Tomonaga-Luttinger liquid theory is well preserved for times up to $Jt = 5\hbar$, although the oscillations are damped under the effect of dissipation.

To obtain a more definite picture, we also consider the

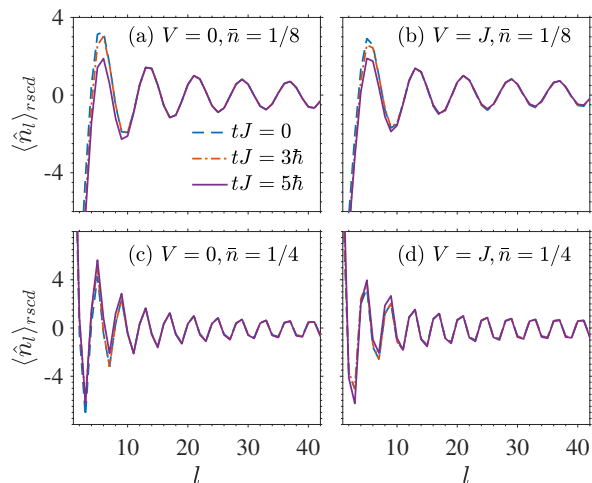


FIG. 6: Rescaled local density $\langle \hat{n}_l \rangle_{\text{rscd}}$ versus site number l , for different times: $tJ = 0$ (blue dashed line), $tJ = 3\hbar$ (orange dash-dotted line) and $tJ = 5\hbar$ (violet solid line). Panels (a) and (b) are for filling $\bar{n} = 1/8$ ($L = 88, N = 11$), $V = 0$ and $V = J$; (c) and (d) are for filling $\bar{n} = 1/4$ ($L = 84, N = 21$), $V = 0$ and $V = J$. For all system parameters and times considered, the bulk of the evolved profiles can be collapsed into the corresponding initial density profile. Results obtained via MPS simulations using the same parameters as in Fig. 5.

evolution of the density-density correlations, $\langle \hat{n}_l \hat{n}_{l+d} \rangle - \langle \hat{n}_l \rangle \langle \hat{n}_{l+d} \rangle$. Just as we did in our study of the results from adiabatic elimination, we first take a look at these correlations for short to intermediate distances. One sees here too, from Fig. 7, that spatial oscillations present initially in the Tomonaga-Luttinger liquid correlations are preserved for a certain time, but are damped out under the effect of dephasing. One can further notice a slow build-up of the correlations for short distances and hints of a breakdown of the algebraic character propagating towards larger distances as time goes on. This behavior is clearly reminiscent of the evolution identified for the corresponding correlations within adiabatic elimination. However, as expected, the time scales are different. While from adiabatic elimination, the oscillations appear to have totally vanished by $Dt \approx 10$, when the evolution is carried out using MPS, properly taking in account the initial coherence and the interaction, oscillations are still present, as seen from Fig. 7, at $Dt \approx 100$ (corresponding here to $tJ = 5\hbar$).

Considerable information can be further gained by considering how the spatial algebraic decay of the density-density correlations is affected by dephasing. Before analyzing the evolution of this decay as function of time, we first study the structure of the initial correlations. In Fig. 8, we show that for various starting locations, l , the correlations are in very good agreement if the initial sites correspond to a maximum of the density profile near the center of the lattice. In particular, we find that the exponent associated with the correlations decay agrees

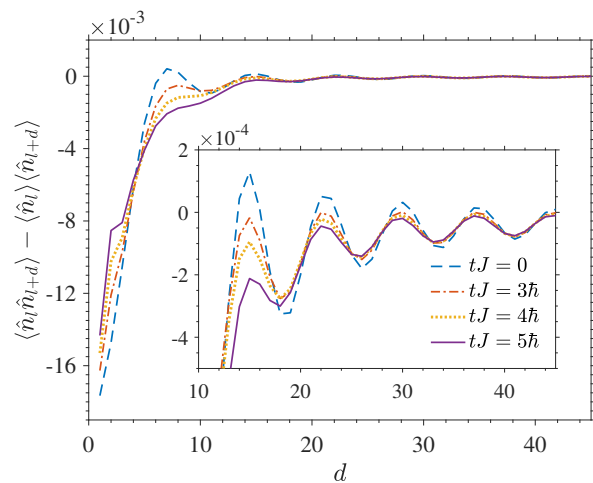


FIG. 7: Density-density correlation $\langle \hat{n}_l \hat{n}_{l+d} \rangle - \langle \hat{n}_l \rangle \langle \hat{n}_{l+d} \rangle$ as a function of distance d ($l = 37$) for $L = 88, N = 11, V = J$ and $\hbar\gamma = 0.05J$. Times considered: $tJ = 0$ (blue dashed line), $tJ = 3\hbar$ ($Dt = 60$, orange dash-dotted line), $tJ = 4\hbar$ ($Dt = 80$, yellow dotted line) and $tJ = 5\hbar$ ($Dt = 100$, violet solid line). Inset: the spatial oscillations of the Tomonaga-Luttinger correlations are damped under the effect of dephasing. Results obtained via MPS simulations using the same parameters as in Fig. 5.

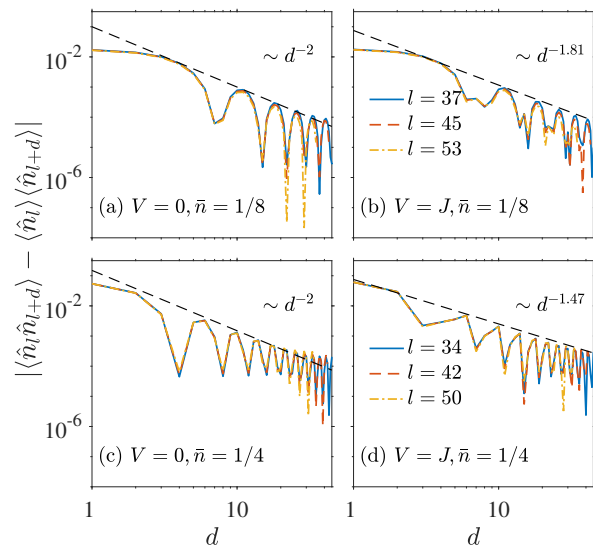


FIG. 8: Absolute value of the initial density-density correlations $|\langle \hat{n}_l \hat{n}_{l+d} \rangle - \langle \hat{n}_l \rangle \langle \hat{n}_{l+d} \rangle|$ as a function of distance d for three different locations. Panels (a) and (b) are for filling $\bar{n} = 1/8$ ($L = 88, N = 11$), $V = 0$ and $V = J$; (c) and (d) are for filling $\bar{n} = 1/4$ ($L = 84, N = 21$), $V = 0$ and $V = J$. As well known from Tomonaga-Luttinger theory, the exponent η in $d^{-1/\eta}$ is function of the filling and interaction strength. Results obtained from MPS simulations using the same parameters as in Fig. 5.

with the value expected from Tomonaga-Luttinger theory [36], even though for the largest distances considered finite size effects are noticeable.

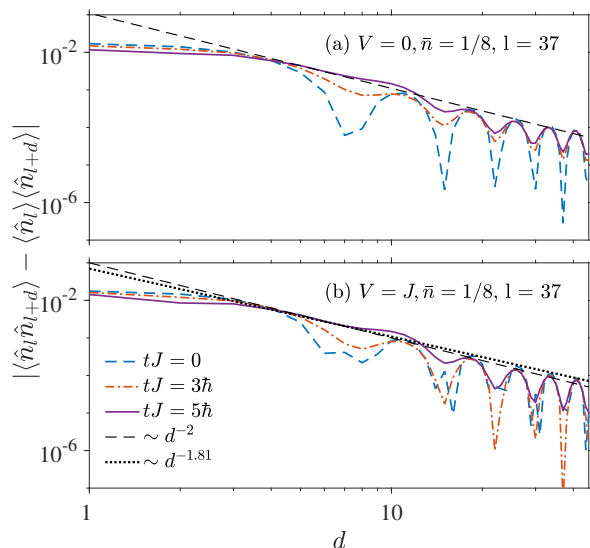


FIG. 9: Absolute value of the density-density correlations $|\langle \hat{n}_l \hat{n}_{l+d} \rangle - \langle \hat{n}_l \rangle \langle \hat{n}_{l+d} \rangle|$ as a function of distance d for $\bar{n} = 1/8$ ($L = 88$, $N = 11$) at three times: $tJ = 0$ (blue dashed line), $tJ = 3\hbar$ (orange dash-dotted line) and $tJ = 5\hbar$ (violet solid line). Panel (a): $V = 0$, panel (b): $V = J$. For all panels $\hbar\gamma = 0.05J$. Results obtained via MPS simulations using the same parameters as in Fig. 5.

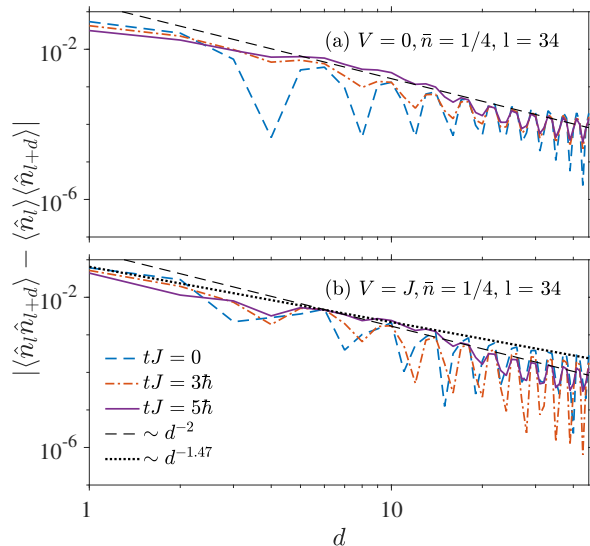


FIG. 10: Absolute value of the density-density correlations $|\langle \hat{n}_l \hat{n}_{l+d} \rangle - \langle \hat{n}_l \rangle \langle \hat{n}_{l+d} \rangle|$ as a function of distance d for $\bar{n} = 1/4$ ($L = 84$, $N = 21$) at three times: $tJ = 0$ (blue dashed line), $tJ = 3\hbar$ (orange dash-dotted line) and $tJ = 5\hbar$ (violet solid line). Panel (a): $V = 0$, panel (b): $V = J$. For all panels $\hbar\gamma = 0.05J$. Results obtained via MPS simulations using the same parameters as in Fig. 5.

We are now in a position to investigate the evolution of the tail of the density-density correlations considering both fillings $\bar{n} = 1/8$ and $\bar{n} = 1/4$ and interaction strengths $V = 0$ and $V = J$. In all cases displayed in

Figs. 9 and 10, one sees that the amplitude of the correlations flattens over time and that this flat region grows. This result hints at the existence of the second regime identified within adiabatic elimination, described using Eq. (9), where a featureless region propagates diffusively through the system. We also notice that for larger distances the exponent associated with the algebraic decay seems, in some cases, to change as dephasing sets in. This is particularly noticeable in Fig. 10(b), for $\bar{n} = 1/4$ and $V = J$, where the initial decay in $d^{-1.47}$ changes with time and appears to adopt the scaling form d^{-2} . A similar situation likely occurs for $\bar{n} = 1/8$ and $V = J$ shown in Fig. 9(b); however, in this case the initial algebraic behavior is in $d^{-1.81}$ so the evolution towards d^{-2} is much harder to confidently ascertain. In the absence of interaction, the decay remains proportional to d^{-2} as predicted by Eq. (8). These results are therefore in agreement with the regimes predicted from adiabatic elimination.

V. CONCLUSIONS

We considered a system of interacting bosons under the effect of dephasing. The system starts as a Tomonaga-Luttinger liquid and then, due to dephasing, heats up. We investigated the quantum dissipative evolution of this system using an approach based on adiabatic elimination and counterchecked our analytical findings by conducting matrix product states simulations.

We found the dephasing to act in two concurring ways: at short to intermediate times, the oscillatory nature of both the density profile and density-density correlations damps out, but their overall algebraic decay, as expected for a Tomonaga-Luttinger liquid, is maintained. However, dephasing is found to alter the interaction and filling-specific exponent associated with the initial algebraic decay. In fact, the correlations scaling, while remaining algebraic, evolves towards the exponent expected for a non-interacting system. Then, at larger times, the algebraic scaling diffusively melts away and is replaced by featureless correlations as expected in the infinite temperature state.

Our work shines a different light on the persistence of universal behaviors in strongly interacting systems under the effect of dissipation, a difficult but important subject that will surely benefit greatly from further refinements of both the theoretical tools and experimental setups in coming years.

Acknowledgement

We thank V. Balachandran, M. Buchhold, S. Diehl, G. Kocher and J. Marino for fruitful and enlightening discussions. The computational work for this article was partially done on resources of the National Supercomputing Centre, Singapore [38]. D.P. acknowledges support from Ministry of Education of Singapore

AcRF MOE Tier-II (project MOE2018-T2-2-142). C.K. acknowledges funding from the Deutsche Forschungsgemeinschaft (DFG, German Research Foundation) under project number 277625399 - TRR 185 (B4) and project number 277146847 - CRC 1238 (C05) and under Ger-

many's Excellence Strategy Cluster of Excellence Matter and Light for Quantum Computing (ML4Q) EXC 2004/1 390534769 and the European Research Council (ERC) under the Horizon 2020 research and innovation programme, grant agreement No. 648166 (Phonton).

-
- [1] S. Sachdev, *Quantum phase transition* (Cambridge University Press, 1999).
- [2] T. Giamarchi, *Quantum Physics in One Dimension* (Oxford University Press, Oxford, 2004).
- [3] M. Buchhold and S. Diehl, *Phys. Rev. A* **92**, 013603 (2015).
- [4] L. M. Sieberer, M. Buchhold, and S. Diehl, *Reports on Progress in Physics* **79**, 096001 (2016).
- [5] A. Kamenev, *Field Theory of Non-Equilibrium Systems* (Cambridge University Press, 2011).
- [6] A. Bácsı, C. Moca, and B. Dóra, arxiv:1911.11602 (2019).
- [7] Y. S. Patil, S. Chakram, and M. Vengalattore, *Phys. Rev. Lett.* **115**, 140402 (2015).
- [8] H. P. Lüschen, P. Bordia, S. S. Hodgman, M. Schreiber, S. Sarkar, A. J. Daley, M. H. Fischer, E. Altman, I. Bloch, and U. Schneider, *Phys. Rev. X* **7**, 011034 (2017).
- [9] R. Bouganne, M. B. Aguilera, A. Ghermaoui, J. Beugnon, and F. Gerbier, *Nature Physics* **16**, 21 (2020).
- [10] N. Malossi, M. M. Valado, S. Scotto, P. Huillery, P. Pillet, D. Ciampini, E. Arimondo, and O. Morsch, *Phys. Rev. Lett.* **113**, 023006 (2014).
- [11] M. M. Valado, C. Simonelli, M. D. Hoogerland, I. Lesanovsky, J. P. Garrahan, E. Arimondo, D. Ciampini, and O. Morsch, *Phys. Rev. A* **93**, 040701 (2016).
- [12] R. Gutiérrez, C. Simonelli, M. Archimi, F. Castellucci, E. Arimondo, D. Ciampini, M. Marcuzzi, I. Lesanovsky, and O. Morsch, *Phys. Rev. A* **96**, 041602 (2017).
- [13] S. Dürr, J. J. García-Ripoll, N. Syassen, D. M. Bauer, M. Lettner, J. I. Cirac, and G. Rempe, *Phys. Rev. A* **79**, 023614 (2009).
- [14] J. J. Garca-Ripoll, S. Dürr, N. Syassen, D. M. Bauer, M. Lettner, G. Rempe, and J. I. Cirac, *New Journal of Physics* **11**, 013053 (2009).
- [15] D. Poletti, J.-S. Bernier, A. Georges, and C. Kollath, *Phys. Rev. Lett.* **109**, 045302 (2012).
- [16] Z. Cai and T. Barthel, *Phys. Rev. Lett.* **111**, 150403 (2013).
- [17] D. Poletti, P. Barmettler, A. Georges, and C. Kollath, *Phys. Rev. Lett.* **111**, 195301 (2013).
- [18] B. Sciolla, D. Poletti, and C. Kollath, *Phys. Rev. Lett.* **114**, 170401 (2015).
- [19] S. Wolff, J.-S. Bernier, D. Poletti, A. Sheikhan, and C. Kollath, *Phys. Rev. B* **100**, 165144 (2019).
- [20] M. Medvedyeva, T. Prosen, and M. Žnidarič, *Phys. Rev. B* **93**, 094205 (2016).
- [21] B. Everest, I. Lesanovsky, J. P. Garrahan, and E. Levi, *Phys. Rev. B* **95**, 024310 (2017).
- [22] B. Olmos, I. Lesanovsky, and J. Garrahan, *Phys. Rev. Lett.* **109**, 020403 (2012).
- [23] I. Lesanovsky and J. P. Garrahan, *Phys. Rev. Lett.* **111**, 215305 (2013).
- [24] S. R. White, *Phys. Rev. Lett.* **69**, 2863 (1992).
- [25] U. Schollwöck, *Annals of Physics* **326**, 96 (2011), january 2011 Special Issue.
- [26] F. Verstraete, M. Popp, and J. I. Cirac, *Phys. Rev. Lett.* **92**, 027901 (2004).
- [27] M. Zwolak and G. Vidal, *Phys. Rev. Lett.* **93**, 207205 (2004).
- [28] A. J. Daley, *Advances in Physics* **63**, 77 (2014), <http://dx.doi.org/10.1080/00018732.2014.933502> .
- [29] L. Bonnes and A. M. Läuchli, arXiv:1411.4831 (2014).
- [30] J.-S. Bernier, R. Tan, L. Bonnes, C. Guo, D. Poletti, and C. Kollath, *Phys. Rev. Lett.* **120**, 020401 (2018).
- [31] H. P. Breuer and F. Petruccione, *The theory of open quantum systems* (Oxford University Press, Oxford, 2002).
- [32] V. Gorini, A. Kossakowski, and E. C. G. Sudarshan, *Journal of Mathematical Physics* **17**, 821 (1976), <https://aip.scitation.org/doi/pdf/10.1063/1.522979> .
- [33] G. Lindblad, *Commun. Math. Phys.* **48**, 119 (1976).
- [34] H. Pichler, A. J. Daley, and P. Zoller, *Phys. Rev. A* **82**, 063605 (2010).
- [35] F. Gerbier and I. Castin, *Phys. Rev. A* **82**, 013615 (2010).
- [36] T. Hikihara and A. Furusaki, *Phys. Rev. B* **63**, 134438 (2001).
- [37] W. Janke and T. Sauer, *Physics Letters A* **165**, 199 (1992).
- [38] <https://www.nscg.sg> .